

Introduction: Overview of Neuronal Signaling

The transmission of information in neuronal networks through both electrical and chemical mechanisms is a fundamental neurobiological principle. Incoming signals are received from other neurons at synapses, commonly located on dendritic spines upon membrane protrusions surrounding the cell body (soma) known as dendrites. Presynaptic cells release neurotransmitters into the synaptic cleft, wherein they bind to specific receptors on the postsynaptic dendritic membrane. Depending on the nature of the neurotransmitter and receptor, binding may result in a depolarization or hyperpolarization of the membrane from the resting membrane potential (RMP). The RMP is commonly located at approximately -65 to -70 mV relative to the outside of the cell, though the magnitude varies between neuronal subtypes, as well as between neurons and other excitable cells. Depolarizing currents result from the influx of positive ions or efflux of negative ions and make the interior of the cell more positive, while the cause and effect of hyperpolarizing currents is the opposite. The magnitude of individual depolarizing and hyperpolarizing currents is a function of the concentration of neurotransmitter released into the synapse, the density of receptors present on the postsynaptic cell, the binding kinetics and reuptake/degradation rate of the neurotransmitter once in the synapse, the electrochemical concentration gradients of the ions on either side of the membrane, and the permeability of the channel to a given ion in its various conformational states. Ionotropic receptors are ion channels which contain transmitter binding sites and respond directly to the binding action of transmitter. These receptors are often responsible for rapid responses to transmitter influx into the synapse. Metabotropic receptors, however, mediate more chronic cellular effects and are often coupled to second messenger signal transduction pathways, regulating synthesis of cyclic adenosine monophosphate (cAMP), or inositol triphosphate (IP₃) and diacylglycerol (DAG), or controlling calcium influx, which in turn mediates numerous cellular pathways [1].

Once currents have been initiated in dendritic compartments, they travel within the neuronal soma, experiencing a reduction in magnitude of the corresponding voltage as a result of the length constant of the neuronal environment. This quantity is related to the various passive electrical properties of the membrane. Regenerative signals known as action potentials have been shown to be induced in certain dendritic compartments as well [2]. Upon traveling through the soma, the voltage signals resulting from postsynaptic currents reach the axon hillock, the point at which signals are spatially and temporally integrated. If a given integrated signal exceeds the threshold value of the neuron, voltage-gated ion channels rapidly open in the axonal membrane. These channels are typically permeable to sodium, though calcium-mediated signals have been shown to exist in cardiac cells. Both sodium and calcium ions are in much higher concentrations in the extracellular environment, and, coupled with the attractive negative electrical potential inside the cell, due largely to the presence of organic anions, these cations flow rapidly into the cell [1].

Local opening of voltage-gated ion channels depolarizes a small region of the axonal membrane with a sufficient magnitude to open voltage-gated channels in neighboring downstream axonal regions. The refractory period entered by previously activated voltage-gated channels prevents propagation of the signal back toward the soma. By this mechanism, the action potential is regenerative and maintains a fixed magnitude down the length of the axon. Myelination of axonal fibers and the resultant transition to saltatory conduction mechanisms allows the action potential to be conducted without regeneration in myelinated regions. Unmyelinated nodes of Ranvier are sufficiently close together to regenerate the action potential amplitude to its normal magnitude while significantly increasing transmission velocities.

Upon arriving at the end of the axon, the electrical signal enters the synaptic terminals, where the neuron serves as a presynaptic fiber, forming synapses with postsynaptic neurons. The voltage signal at this location serves to open voltage-gated calcium ion channels, of which there are numerous types expressed in different cells with varying properties [3]. Calcium serves as the primary trigger for synaptic transmission. Upon entering the presynaptic terminal, calcium binds to the protein synaptotagmin within complexes known as v-SNARES, which are associated with t-SNARE complexes on the presynaptic membrane in the docked conformation. Upon binding to calcium, synaptotagmin experiences a conformational change that facilitates vesicle fusion with the membrane, thereby releasing a quantum of neurotransmitter into the synaptic cleft. Depending on the nature of the transmitter, the signal is deactivated upon reuptake by neurons and glial cells or upon degradation by synaptic enzymes [1].

The following model incorporates the fundamental principles to reproduce the above signaling mechanisms of neurons by utilizing previously developed and validated kinetic models for AMPA, NMDA, and GABA_A receptors, Hodgkin-Huxley formalisms for voltage-gated action potential propagation along the axon and subsequent calcium influx at the presynaptic terminal, and a kinetic model to couple calcium influx to transmitter release. Once this model has been established, a new kinetic model is presented to introduce the μ opioid receptor, the primary binding partner of morphine associated with the development of tolerance [4]. This model takes into account two major established acute responses to opioid binding: presynaptic inhibition of calcium influx [5, 6] and activation of G protein-coupled inward-rectifying potassium ion channel current [7-9], and a longer-term postsynaptic reduction in AMPA receptor concentration via internalization [10, 11]. Additionally, parameters are introduced to reflect the development of tolerance due to prolonged opioid exposure and subsequent recovery [12-15].

Postsynaptic Receptors and Receptor Binding Kinetic Models

Receptors for signal transduction pathways may be found not only in dendritic spines, but also along the soma, the axon, or the presynaptic terminals. In many cases, non-dendritic receptors serve to modulate signaling cascades rather than to initiate action potentials. For the purposes of capturing the important cellular mechanisms leading to signal propagation, three receptor subclasses are considered in the dendritic compartment, aside from the opioid receptors, which are considered later. Two of the major neurotransmitters governing information transfer in the brain

are glutamate and γ -aminobutyric acid (GABA). The former serves as the major excitatory neurotransmitter, while the latter serves an inhibitory role by producing hyperpolarizing currents [1]. Ionotropic channels are considered for the generation of dendritic signals using previously developed simple kinetic models and a gain partially reflecting the integration of signals from various dendritic compartments, and partially as a consequence of the change in units for conductances and currents from nS and pA to mS/cm² and μ A/cm². Though the effects of membrane length and time constants, as well as spatial and temporal integration of signals, are of interest in understanding neurocomputational dynamics, these effects are not explicitly considered here due to lack of computational power. Thus, a single dendritic compartment is considered, as is commonly used in neuronal modeling, containing densities of AMPA, NMDA, and GABA_A ionotropic channels.

AMPA

The α -amino-3-hydroxy-5-methyl-4-isoxazolepropionic acid (AMPA) channel is a simple ligand-gated ion channel. Though more complicated kinetic models exist for each of the ionotropic channels considered here, the fundamental dynamics of each of the ion channels may be reproduced using a two-state kinetic scheme of the form [16]:

$$\frac{dr}{dt} = \alpha[T](1 - r) - \beta r$$

In this differential equation, r is a gating variable representing the fraction of open channels, and the constants α and β represent ungating of closed channels and gating of open channels, respectively. For the AMPA model, experimental data described in [16] yielded $\alpha = 1.1 \times 10^6 \text{ M}^{-1} \text{ s}^{-1}$ and $\beta = 190 \text{ s}^{-1}$. From a given value of r , the current flowing through AMPA receptors is given by:

$$I = g_{\text{AMPA},\text{max}} r (V - E_{\text{AMPA}})$$

Where g is the maximal AMPA conductance is 0.001 nS, and $E_{\text{AMPA}} = 0 \text{ mV}$ is the AMPA reversal potential.

GABA_A

The ionotropic GABA_A receptor is treated identically to the AMPA receptor, and is found to have gating constants of $\alpha = 5 \times 10^6 \text{ M}^{-1} \text{ s}^{-1}$ and $\beta = 180 \text{ s}^{-1}$, a maximal conductance of 0.25 nS, and a reversal potential of -80 mV.

NMDA

The N-methyl-D-aspartate (NMDA) receptor is slightly more complicated than the previous two ionotropic receptors due to the presence of a Mg^{2+} ion which blocks the channel, and is only removed by depolarization. Thus, the NMDA receptor requires previous depolarization due to the action of, for example, AMPA receptors, which also respond to glutamate, before they can allow current flow. This magnesium ion dependence is introduced in the $B(V)$ term of the current:

$$\frac{dr}{dt} = \alpha[T](1 - r) - \beta r \text{ and } I = g_{\text{NMDA},\text{max}} r B(V) (V - E_{\text{NMDA}})$$

Gating parameters for the NMDA receptor are found to be $\alpha = 7.2 \times 10^4 \text{ M}^{-1} \text{ s}^{-1}$ and $\beta = 6.6 \text{ s}^{-1}$, the reversal potential is 0 mV, the maximal conductance is 0.01 nS and the magnesium dependence is given by:

$$B(V) = (1 + \exp(-0.062V) [Mg^{2+}]/3.57)^{-1}$$

The extracellular magnesium concentration which enters into the above equation is taken as 1 mM. Leakage channels are also included in the dendritic compartment to allow the spines to return to resting membrane potential once current has stopped flowing. These channels are discussed further in the next section.

Ion Channel Dynamics

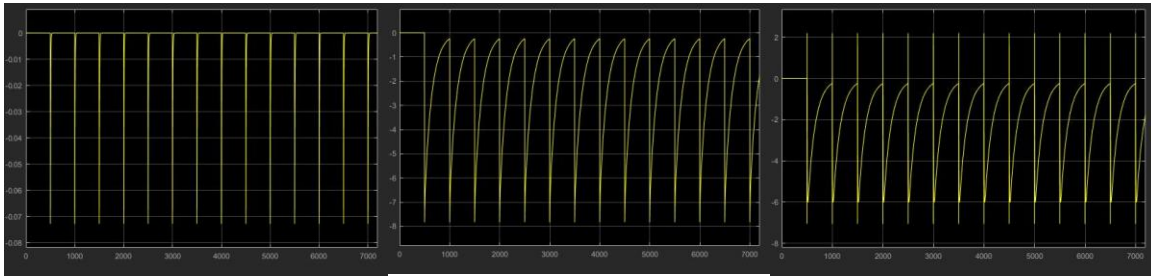


Figure 1. AMPA (left) and NMDA (middle) responses to 1 M glutamate pulses. Right contains the GABA_A response to a 0.01 M pulse, though the dynamics are integrated with the glutamatergic responses. Time axis is in milliseconds and current axis is in pA.

The above figures display the dendritic current dynamics in response to a 1 M pulse of glutamate with or without a 0.01 M pulse of GABA every 500 msec. The rapid time course of the AMPA response and the slower time course of the NMDA response are commonly observed and are characteristic of the given receptors. It should be noted that the dynamics exhibited by GABA stimulation reflect not only the action of GABA but also coupling to the local activation of AMPA and NMDA channels, which changes local membrane potential, thereby disrupting GABA currents. In real neurons, GABA and glutamate receptors are not this close in proximity, so dynamics like this will not be observed. For this reason, as well as the fact that there is no documented evidence that activation of opioid receptors interferes with GABAergic reception, these receptors are not considered beyond implementation with the Hodgkin-Huxley model.

The Hodgkin-Huxley Model and Action Potential Propagation

The electrical properties of voltage-gated channel-dependent action potential conduction were first explained in a mathematical model by Hodgkin and Huxley in 1952. The mechanism of the Hodgkin-Huxley model and relevant equations have been previously detailed in another report, and are summarized here. The model is constructed as a system of four coupled differential equations, three of which serve as the voltage-dependent “gating variables” for the sodium and potassium channels that govern action potential generation and propagation in the giant squid axon used by Hodgkin and Huxley. These variables range between 0 and 1 and reflect opening of

molecular gates, allowing current to flow through. The sodium channel gating is modeled by the term m^3h , where m is the activation variable, which increases upon depolarization, and h acts to inactivate the channel. The potassium channel is modeled by n^4 , and inactivates more slowly upon the membrane returning to RMP. Each gating variable can be expressed with analogous differential equations to those presented for r in the ionotropic receptor equations, with the amendment that the gating constants are now functions of the membrane voltage of the cell. These are fit to the following functional forms for the three gating variables [17]:

$$\alpha_n(V) = \frac{0.01(10 - V)}{\exp\left(\frac{10 - V}{10}\right) - 1} \quad \beta_n(V) = 0.125\exp(-V/80)$$

$$\alpha_m(V) = \frac{0.1(25 - V)}{\exp\left(\frac{25 - V}{10}\right) - 1} \quad \beta_m(V) = 4\exp(-V/18)$$

$$\alpha_h(V) = 0.07\exp(-V/20) \quad \beta_h(V) = \frac{1}{\exp\left(\frac{30 - V}{10}\right) + 1}$$

In the above equations, V , denotes the deviation from the resting membrane potential, rather than the absolute value of the membrane voltage. The resting potential is taken as -65 mV.

The final equation is obtained by analyzing the axon as an electrical circuit, and solving for the dV/dt term to obtain the membrane voltage as the signal propagates:

$$\frac{dV}{dt} = \frac{-1}{C_m} [I_{\text{external}} + I_{\text{Leak}} + I_{\text{Na}^+} + I_{\text{K}^+}]$$

Here, C_m is the membrane capacitance (1 $\mu\text{F}/\text{cm}^2$), and the total current flow consists of external current sources (e.g. patch clamping, current influx from dendritic compartments), current due to sodium influx and potassium efflux, and a leakage current due to constitutively open ion channels that allow the membrane to return to RMP. Each of the currents can be modeled by $I = \bar{g}_{\text{max}}x(V - E_x)$, where g is the maximal channel conductance, x is a gating function (specified above for sodium and potassium, and simply equal to 1 for the leakage current), and E_x denotes the Nernst potential, also known as the reversal potential, at which the current will switch directions due to changes in the net electrochemical gradient balance between electric charge and concentration gradients. Reversal potentials are 0 mV for leak, +55 mV for Na^+ , and -77 mV for K^+ . Maximal conductances are 40 mS/cm^2 , 35 mS/cm^2 , and 0.3 mS/cm^2 for sodium, potassium, and the leak current, respectively. The Hodgkin-Huxley model is employed here to propagate the action potential to the presynaptic terminals. Due to the success of the Hodgkin-Huxley model in explaining action potential generation, similar models following the ‘‘Hodgkin-Huxley formalism’’ have been used to capture other voltage-gated cellular processes, and have been found to capture these intracellular dynamics quite well, along with other modeling schemes including kinetic and thermodynamic models [18].

Dynamics of the Hodgkin-Huxley Model

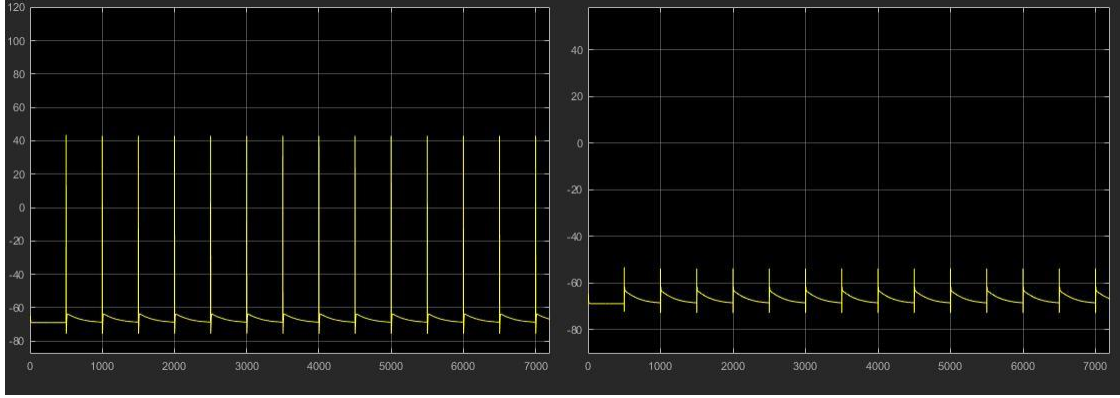


Figure 2. Hodgkin-Huxley model in response to the dendritic current influx from 1 M glutamate pulses with (right) and without (left) coincident GABA pulses. In the right-hand figure, the membrane voltage almost reaches the threshold value, but is not large enough, so an action potential is not initiated. Time axis is in ms and voltage axis is in mV.

As shown above, the Hodgkin-Huxley model reproduces the expected action potential dynamics with a large enough glutamatergic stimulus, and GABA can serve to prevent action potential generation by hyperpolarizing the cell. Beyond this section, the effects of GABA in regulating action potential initiation and subsequent transmitter release are not considered, as it is simply a sum of the currents leaving the dendritic compartment and does not contribute much to the effects of opioid receptors and the development of tolerance. Further analysis of the behavior of the Hodgkin-Huxley model can be found in the previous discussion.

Calcium Influx and Exocytosis at the Synaptic Terminal

Upon reaching the synaptic terminal, the voltage signal serves to open voltage-gated calcium channels, which may in turn initiate the neurotransmitter release process by binding to synaptotagmin and promoting vesicle fusion [1]. Calcium influx is modeled by a Hodgkin-Huxley-like m^2h gating model developed for thalamic reticular neurons in [19]. The calcium current flowing into the cell is given by:

$$I_T = g_{Ca,max} m^2 h (V - E_{Ca})$$

The maximal calcium conductance is adjusted to 17.5 mS/cm^2 in order to elicit calcium pulses on the order of 10^{-7} to $10^{-8} \text{ } \mu\text{A/cm}^2$ and cause release of significant transmitter concentrations. The gating variables are modeled by the equations:

$$\frac{dm}{dt} = -\frac{1}{\tau_m(V)} [m - m_\infty(V)] \text{ and } \frac{dh}{dt} = -\frac{1}{\tau_h(V)} [h - h_\infty(V)]$$

The time constants and maximum values are given by:

$$m_\infty(V) = (1 + \exp\left(-\frac{V+52}{7.4}\right))^{-1} \text{ and } \tau_m(V) = 0.44 + 0.15 / \left\{ \exp\left(\frac{V+27}{10}\right) + \exp\left(-\frac{V+102}{15}\right) \right\}$$

$$h_\infty(V) = (1 + \exp\left(\frac{V+80}{5}\right))^{-1} \text{ and } \tau_h(V) = 22.7 + 0.27 / \left\{ \exp\left(\frac{V+48}{4}\right) + \exp\left(-\frac{V+407}{50}\right) \right\}$$

The resultant calcium current is then converted to a change in calcium concentration by the relation $[Ca^{2+}] = -\frac{k}{2Fd}I_T$, where F is the Faraday constant (96489 C/mol), d is the depth of a thin shell beneath the membrane (1 μ m), k is a unit conversion factor equal to 0.1 to yield $[Ca^{2+}]$ in millimolar, and I_T is the calcium current. Calcium efflux is also considered by a saturating pump which follows the equation:

$$\frac{d[Ca^{2+}]}{dt} = -\frac{K_T[Ca^{2+}]}{K_d + [Ca^{2+}]}$$

The dissociation constant, K_d , is set to 10^{-4} mM, and K_T is taken as 10^{-4} mM/ms in order to remove calcium in the millisecond range.

This calcium influx is then coupled to a Markov kinetic model [20] for presynaptic calcium dynamics, in which calcium ions reversibly bind to the synaptotagmin/vesicles containing neurotransmitter, and the activated vesicle then irreversibly fuses with the membrane. This portion of the model is adapted from [16], which instead considers multiple reversible binding events (i.e. calcium to some calcium-binding protein, which is in turn activated and may then bind to the vesicle complex). It is assumed that four calcium ions bind to a molecule of synaptotagmin to trigger release. As the above mechanism is simpler and still accurate, and perhaps reflects intracellular dynamics of transmitter exocytosis more accurately, it is used instead. Thus, the calcium dynamics are summarized by the equation:

$$\frac{d[Ca^{2+}]}{dt} = k_{pump} + k_{influx} + k_u[Ca - complex] - k_b[Ca^{2+}]^4[SNARE]$$

The SNARE concentration is held constant at 0.01 mM, as synaptic depletion is not considered, and this value is quite significantly above the calcium concentrations attained by the model.

The bound calcium-SNARE complex kinetics are described by the equation:

$$\frac{d[Ca - complex]}{dt} = -k_u[Ca - complex] + k_b[Ca^{2+}]^4[SNARE] - k_r[Ca - complex]$$

Here, the final term describes the irreversible fusion of a synaptic vesicle with the membrane and exocytosis of transmitter. The constants are taken from [16] as $k_u = .1 \text{ ms}^{-1}$, $k_b = 100 \text{ mM}^{-1} \text{ ms}^{-1}$, and $k_r = 4 \text{ ms}^{-1}$. A quantum of transmitter is assumed to contain an arbitrary number of transmitter molecules, taken to be 10,000. Thus, with the calcium dynamics, the neuronal model without the effects of opioid exposure is complete, reflecting the reception of a signal, transduction to dendritic ion currents, initiation and propagation of an action potential, and subsequent calcium influx and transmitter release.

Dynamics of Calcium-Dependent Transmitter Release

The following figures display the calcium concentration in the synaptic terminals and the transmitter concentration in the synapse over the course of the 7200 ms in the above examples. It is apparent that the pump specified in [18] does not promote complete removal of the calcium influx, leading to monotonically increasing calcium concentrations as the simulation progresses. Though this does not reflect realistic dynamics of the neuron, it is still useful in examining how the presence of opioid receptor activation alters calcium dynamics and subsequent transmitter

release. Similarly, transmitter removal in the form of uptake or degradation from the synapse was not considered, and so this concentration also increases throughout the simulation, though this is acceptable as the released transmitter is not part of any feedback loop, and simply serves as a measure of the total response. Both calcium concentrations and transmitter concentrations are extremely low, which may be a consequence of some other part of the model that does not properly fit experimental data. This may be fixed by the scaling of conductances above what was already done, if necessary, though it is still sufficient to examine system dynamics.

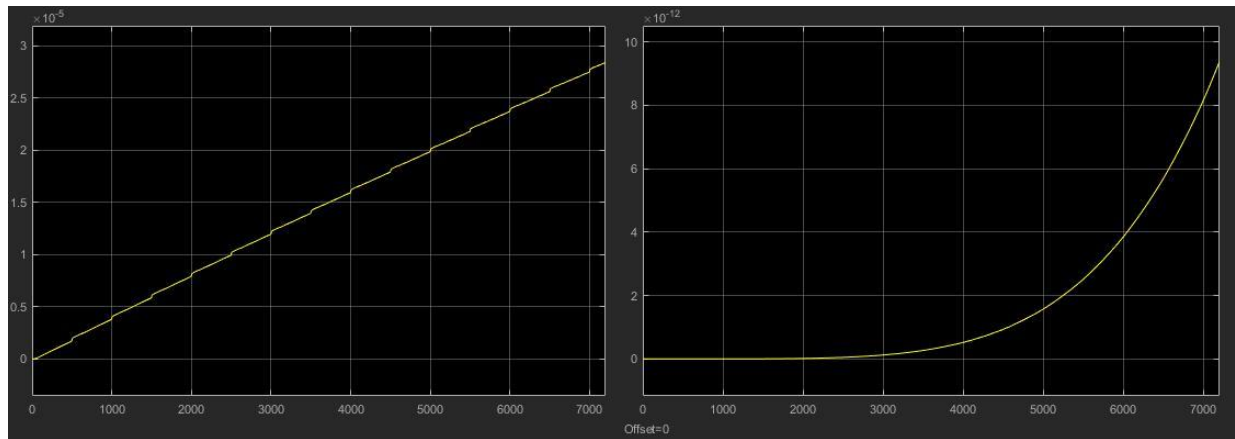


Figure 3. Calcium concentration (left) and total transmitter release (right) of the model without any opioid receptor activation. Time axis is in ms and concentration is in mM.

The μ Opioid Receptor and the Development of Morphine Tolerance

Biological Basis

As tolerance and addiction to opioids is quite a significant medical issue, the structure and function of opioid receptors and their cellular effects upon activation is being heavily researched. At least three different classes of opioid receptors have been found, though other groups have also been recently introduced [12]. Of these, the μ opioid receptor has received the most interest as it has been shown to interact most strongly with morphine, and has also been shown to interact with alcohol, cannabinoids, and nicotine [4]. Opioid receptors have been shown to be expressed in descending pathways which modulate pain, such as the medulla locus coeruleus and periaqueductal gray area, as well as limbic, midbrain, and cortical structures [12]. As this topic is a current area of research, there is a lack of definitive conclusive evidence regarding the specific effects of differential signaling due to variation of binding partners and coupling to intracellular signaling events, especially in the area of the development of tolerance and addiction. However, the basis of opioid receptor activation and its acute effects in modulating transmitter release have been well-established.

All classes of opioid receptors are coupled to G-protein signaling systems (GPCRs) and are associated with G_i inhibitory α subunits [4]. Once activated, these proteins may dissociate into their functional forms and produce a number of cellular effects [12]. The most well-documented effects of acute opioid channel activation include inhibition of adenylyl cyclase, the enzyme which catalyzes the conversion of ATP to cAMP, and suppression of presynaptic transmitter release,

typically in GABAergic neurons [21], through the inhibition of high-threshold calcium current [5, 6, 22] and activation of G-protein coupled inward-rectifying potassium channels (GIRKs) [7]. μ opioid receptors have also been found to be expressed at some postsynaptic terminals colocalized with AMPA receptors, and activation has been demonstrated to promote decreased density of dendritic spines and internalization of AMPA receptors [10, 23]. Thus, the overall function of activation of opioid receptors on an acute timescale is to suppress neuronal activity in specific neurons by both pre- and postsynaptic mechanisms.

While understanding of the acute effects of opioid receptor activation is important in designing novel therapeutic interventions to promote analgesia, the necessity for developing such interventions is a consequence of the rapid development of tolerance and addiction to agonists of opioid receptors, including morphine [15, 24, 25]. It is in this area that much of the current research regarding these receptors is taking place. As the specific underlying mechanisms governing tolerance have not been completely uncovered, a hypothesis discussed in [26] is used to explain the connection between G-protein activity and the development of tolerance. In this hypothesis, μ opioid receptors undergo rapid desensitization by G-protein-dependent kinase (GRK) phosphorylation. The resensitization of these receptors is then dependent on the endocytosis of the desensitized/phosphorylated receptor into the intracellular environment [14], wherein it is dephosphorylated and may be returned to the surface. There has not been substantial evidence that μ opioid receptors are degraded upon internalization. However, it has been shown that different agonists display large variations in the amount of receptor internalization relative to the amount of phosphorylation, which is also consistent with the observation that agonists vary significantly in the amount of tolerance developed over extended periods of exposure [27]. This has been experimentally characterized by the so-called “RAVE” (“relative activation versus endocytosis”) number, taken as the ratio of receptor activation to internalization initiated by a specific agonist [28]. Agonists such as morphine, which display high RAVE numbers, typically promote the development of opioid tolerance and dependence. This logically follows from the above hypothesis, as increased receptor activity may promote phosphorylation-dependent desensitization but a large RAVE number indicates a lack of subsequent internalization and resensitization, thereby reducing the overall number of active receptors, leading to the development of tolerance.

Model Construction

The previously introduced kinetic model to describe reception, transduction, and propagation of signals, followed by calcium-dependent transmitter release is developed in such a way that most of the important binding targets for μ opioid receptor activation are already present, largely in the form of the calcium pathway and AMPA channels. Introduction of a G protein-dependent potassium channel completes the most well-characterized mechanisms of acute receptor response. Though it has been established that the potassium channels acted on by $G\beta\gamma$ subunits from opioid-dependent pathways are inward-rectifying, this property is not reproduced in the model, as the function of the channel is to hyperpolarize the cell, since the membrane potential does not reach the reversal potential of potassium, so the change in conductance as current flows

the opposite way is not relevant. The μ opioid receptor itself is introduced with four states and a direct coupling to G protein activation, wherein a number of G proteins is activated in proportion to the number of receptors bound to agonists at each time point. The G protein kinetic scheme governs the transduction of the opioid binding signal to the physiological effects. G proteins are deactivated once they interact with a substrate through the hydrolysis of GTP, and for simplicity, it is assumed that the activated G proteins from the μ opioid GPCR are only involved in the events surrounding receptor activation, and that the only G proteins which interact with these substrates come from μ opioid receptor activation. Therefore, G protein levels are increased by agonist binding to the μ receptor, and are decreased as a result of: i) calcium channel inactivation, ii) GIRK channel activation, iii) AMPA channel internalization, and also mediate opioid receptor phosphorylation via GRK activity. Tolerance is then introduced by an additional rate which is dependent on the RAVE parameter of interest for the specific agonist. High RAVE numbers correspond to low levels of endocytosis and resensitization, and thus lead to more rapid tolerance. The rate of internalization is also proportional to the total concentration of phosphorylated receptor. Thus, the kinetic scheme for the receptor is:

$$\begin{aligned}\frac{d[MuR]}{dt} &= -k_p[G][MuR] + k_{dp}[MuR - P] - k_b[MuR][Morph] + k_u[MuR - Morph] + \\ &\quad k_r[MuR - int] \\ \frac{d[MuR - P]}{dt} &= k_p[G][MuR] - k_{dp}[MuR - P] - k_{int}[MuR - P] \\ \frac{d[MuR - Morph]}{dt} &= k_b[MuR][Morph] - k_u[MuR - Morph] \\ \frac{d[MuR - int]}{dt} &= k_{int}[MuR - P] - k_{re}[MuR - int]\end{aligned}$$

For the concentration of activated G protein, assuming that the inactive G protein concentration is not depleted (i.e. there is sufficient available local G protein around the receptor to be activated):

$$\frac{d[G]}{dt} = k_{Gact}[MuR - Morph] - k_{AMPA}[G][AMPA] - k_{GIRK}[G][GIRK] - k_{Ca}[G][Ca\ channel]$$

The concentration of morphine is dependent only on its binding to and unbinding from the receptor, as well as external inputs and outputs. For the purposes of testing the model, morphine is delivered and removed as a pulse, and so explicit biological removal is not considered. Additionally, in order to examine the development of tolerance, morphine is maintained at a constant 10 μ M concentration for most of the analysis.

This also requires the introduction of the complementary terms for the calcium and AMPA currents in their respective differential equations, which are modeled using the same two-state system as those used for postsynaptic ionotropic receptors. For the AMPA channel internalization:

$$\frac{d[AMPA]_{closed}}{dt} = k_{AMPA}[G]([AMPA]_0 - [AMPA]_{closed}) - k_{recovery,AMPA}[AMPA]_{closed}$$

Similarly, the calcium channel dynamics are modeled as:

$$\frac{d[Ca^{2+}]_{closed}}{dt} = k_{Ca}[G]([Ca^{2+}]_0 - [Ca^{2+}]_{closed}) - k_{recovery,Ca}[Ca^{2+}]_{closed}$$

The G protein-regulated potassium channels are activated and opened by transduction pathways associated with opioid receptors, rather than closed or inactivated, and thus the form of the differential equation is opposite:

$$\frac{d[GIRK]_{open}}{dt} = k_{GIRK}[G]([GIRK]_0 - [GIRK]_{open}) - k_{recovery,GIRK}[GIRK]_{open}$$

Fitting of Model Parameters

The rate constants mediating the acute effects of morphine analgesia were introduced first, including the GIRK channel activation and calcium current inhibition. Once these parameters had been established, a second version of the model was created using the same parameters, but without the coupling to the neuron, and with all rate constants scaled by 10^{-3} to convert the time scale from milliseconds to seconds. This allows for the examination of the development of morphine tolerance over the course of hours or days, while the other version is focused primarily on acute effects. The GIRK channel rate constants were taken from those obtained in [29] for ML297, a selective agonist for the same class of channels used by morphine (K_{ir3}) at $10 \mu M$, the same concentration used for morphine in the model. The activation rate parameter was then $1 s^{-1}$ and the inactivation rate constant was $1/12 s^{-1}$. These parameters are found to accurately reproduce the shape of the GIRK current under the same concentration of morphine:

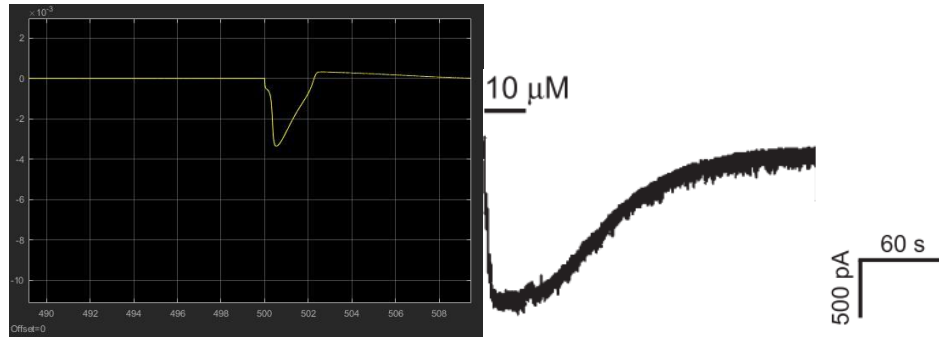


Figure 4. GIRK channel currents in the model and from the reference [29]. Time is in ms and current is in $\mu A/cm^2$.

The conductance used from the Hodgkin-Huxley model was modified to a significantly smaller value ($90 nS/cm^2$) to reflect the smaller channel density of GIRK in comparison to voltage-gated potassium channels mediating the action potential in order to obtain a resulting current on the correct order of magnitude to that in the study ($\sim nA$). As in the calcium and AMPA channels, the maximal conductance is scaled at each time point by the fraction of open channels relative to the total channel concentration, though channel “concentration” is ill-defined as receptor densities are often given over some area of the membrane rather than a volume, so a value of 0.0001 was used, which produced the correct dynamics with the other parameters fit from data. A leak current is also included in the GIRK channel dynamics, as the membrane is expected to return to RMP once GIRK channel activity has been removed. Prolonged exposure to morphine is also found to decrease the magnitude of the resting potential between spikes by small amounts over time.

The rate constants for the calcium current were estimated from [30], who found a median onset time of ~2.5 seconds for the reduction in calcium current under the action of DAMGO, a commonly used opioid receptor agonist which has been shown to exhibit reduced tendency for tolerance. Though a concentration of 1 μM was used in the study, the results here were taken for the 10 μM concentration, since the magnitude of the actual decrement in current varies significantly between receptor subtypes. The $\alpha_{1B} \alpha_2\beta_4$ receptor experiences a decrease by approximately a factor of two, while the $\alpha_{1A} \alpha_2\beta_4$ receptor is only scaled by ~1.4. Parameters were adjusted to yield the following results, which experience a significant reduction in magnitude by approximately 2.5 seconds, consistent with the experimental results, with a ratio of peak currents before and after the reduction of ~5/3, intermediate between the two channel classes. Additionally, the slower time course of channel current recovery in the experimental data is reflected in the slower rate constant in the model.

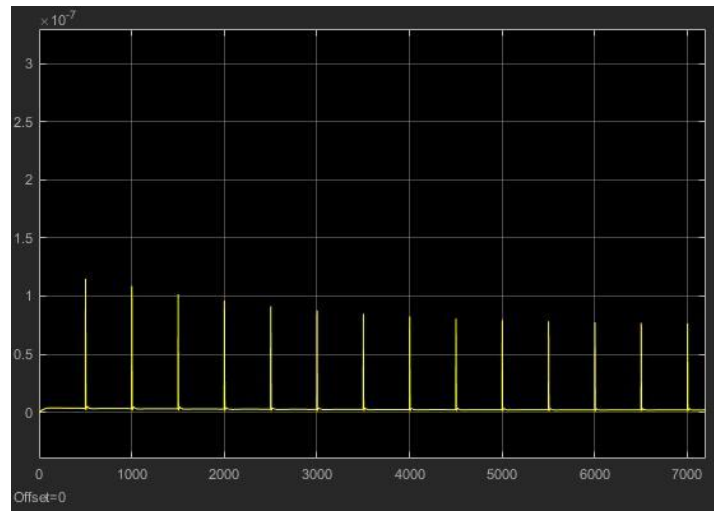


Figure 5. Reduction in calcium current intensity as a result of morphine exposure. The onset time and magnitude are found to be consistent with [30]. Time axis is in ms and current axis is in $\mu\text{A}/\text{cm}^2$.

The effects of both GIRK channel activation and calcium current suppression serve to presynaptically inhibit transmitter release, thereby preventing signal propagation. The implemented morphine model was found to decrease the final synaptic concentration of transmitter by a factor of 4-5 after 7200 msec.

For the purposes of fitting experimental data to more chronic effects of morphine exposure, a second version of the model was employed with each of the above rate constants scaled to the corresponding value with the time measured in seconds, permitting analysis of the development of AMPA internalization and tolerance over the course of a day, rather than a few seconds. The RAVE parameter, which measures the ratio of receptor activation (here, phosphorylation) to internalization, was taken to be 50, within the range of that measured for morphine in [28].

Data from [10] was used to fit the rate constants for AMPA internalization and reduction of dendritic spine density, which, for the purposes of the model, are coupled, since less AMPA receptors has the same effect that reduced dendritic density would. In this study, AMPA receptor

fluorescence was found to be decreased to 80% of its initial value after three hours of chronic morphine exposure, and to 60-65% after one day. The following figure shows that these values are satisfied using an internalization rate constant of 0.0075 s^{-1} and recovery constant of 0.00004 s^{-1} .

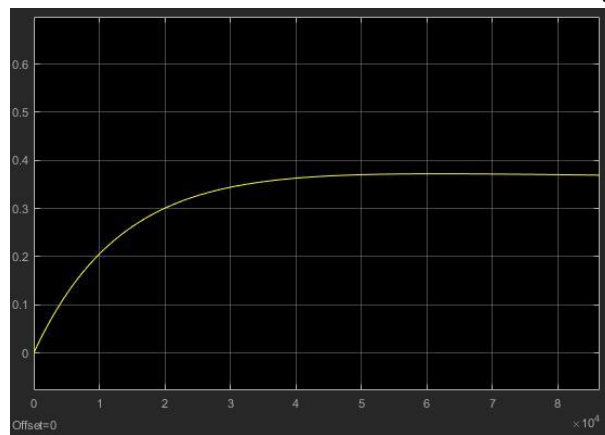


Figure 6. AMPA receptor internalization due to chronic morphine binding to opioid receptors. Time axis is in seconds and the vertical axis is the fraction of inactivated AMPA channels.

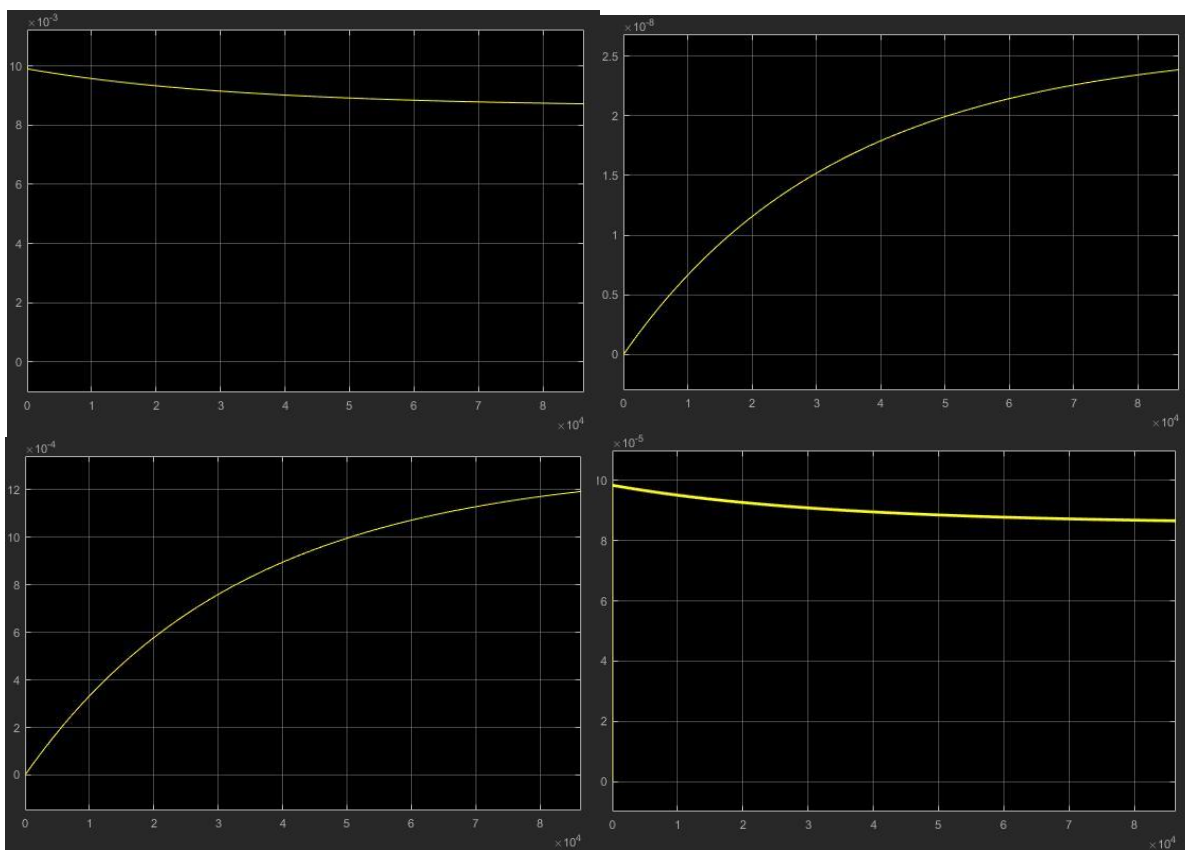


Figure 7. The top left image displays the concentration of free opioid receptors for binding over the course of a day. Going clockwise, the following display internalized receptors, receptors bound to morphine, and phosphorylated. Time axis is in seconds and vertical axis represents concentrations in mM.

The rate constants for the development of tolerance were taken to be: phosphorylation rate constant of 0.001 s^{-1} , dephosphorylation of 10^{-11} s^{-1} , and resensitization of 1 s^{-1} . Since receptor dephosphorylation has not been shown to be a significant recovery mechanism for opioid resensitization, this constant is quite small. Additionally, the rate constants here are consistent with the hypothesis that the limiting factor in receptor recovery is internalization, rather than resensitization once internalized. These constants yield the dynamics in the figure above. By the end of a day, more than 10% of all available opioid receptors are unavailable for binding, which is due most significantly to phosphorylation without subsequent internalization and recovery, consistent with the expectations of the employed hypothesis. As little experimental data is available regarding the actual magnitude of phosphorylated opioid receptors over time, these parameters were estimated based on the rapid development of tolerance over hours to days from chronic morphine exposure [15]. G protein concentrations, while not included above, are found to follow a similar trend to available morphine receptors, as expected. However, the concentration of G proteins is reduced by a factor of $\sim 25\%$ after the first day, which may quite significantly affect the analgesic effect of morphine administration, giving rise to the behavioral effects of tolerance.

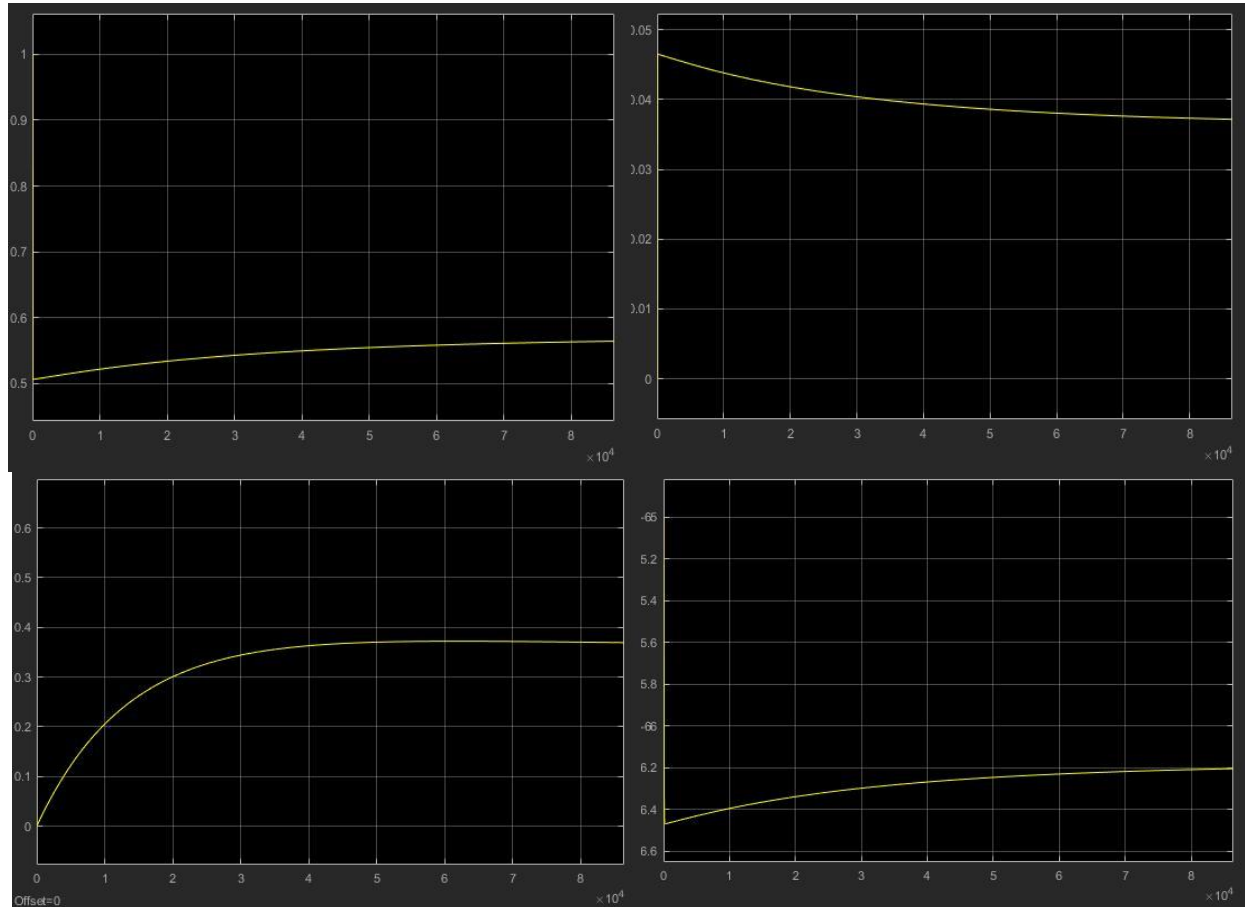
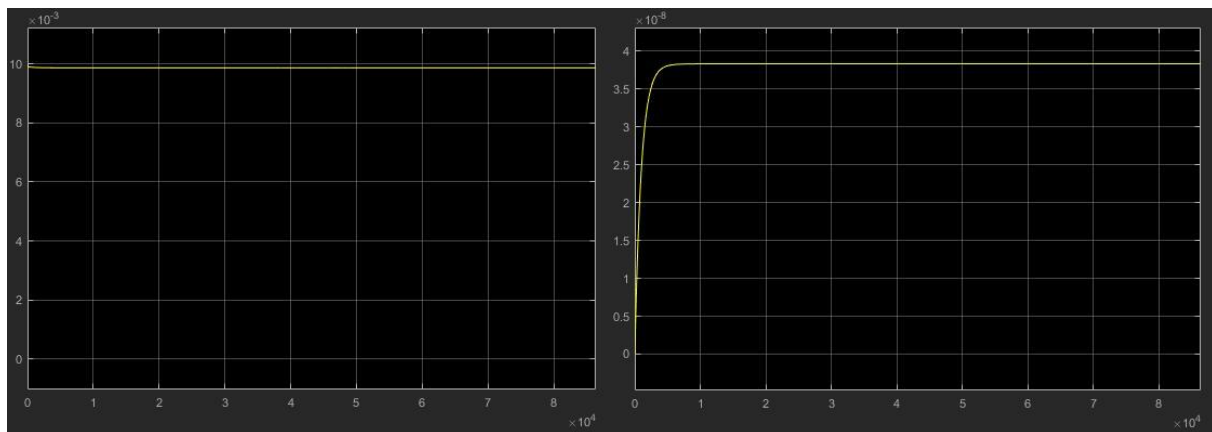


Figure 8. Effect of morphine tolerance on the primary cellular mediators of analgesic effects due to opioid receptor activation. The top left displays the fraction of activated calcium channels as tolerance develops, and going clockwise, the next three contain the fraction of activated GIRK channels, resting membrane potential of the cell (mV), and fraction of internalized AMPA receptors.

The first image in the figure displays a decrease in inactivated calcium channels as a consequence of the reduced synthesis of G proteins from reduced receptor availability. This ultimately leads to increased calcium influx upon conduction of an action potential, and thus, increased exocytosis of neurotransmitter. Increased exocytosis is also a consequence of the reduced fraction of activated GIRK channels, which in turn increases the resting membrane potential of a cell, making the opening of voltage-gated calcium channels more likely upon conduction of an action potential. Finally, the amount of internalized AMPA receptors is beginning to decline at the end of the day by a small amount that will likely increase as the availability of G proteins is further reduced. The slower response of AMPA activity is consistent with the much smaller rate constants mediating the AMPA effects, as well as the fact that AMPA channels are not merely activated or inactivated by G protein-dependent mechanisms, but are internalized and must be returned to the cellular surface or, if they have been degraded, synthesized beginning by the transcription of AMPA genes.

Agonist Effects

In order to highlight the profound influence of functional selectivity of opioid receptors for agonists [27], the RAVE parameter in the opioid tolerance model was set to 1 instead of 50, which is the value in [28] for dihydroxyetorphine (DHE). As evident from the following figure, each of the four possible functional states of the μ opioid receptor rapidly reach their steady-state values and do not deviate from them throughout the duration of the simulation. Consequently, the same is true for the calcium inactivation, GIRK activation, and AMPA internalization. The deviation in steady-state conditions is apparent from the AMPA images in Figure 8 and Figure 10. Clearly more receptors are internalized with a lower RAVE value, and it appears that this increased inactivation of AMPA currents may continue as the one-day time point is passed.



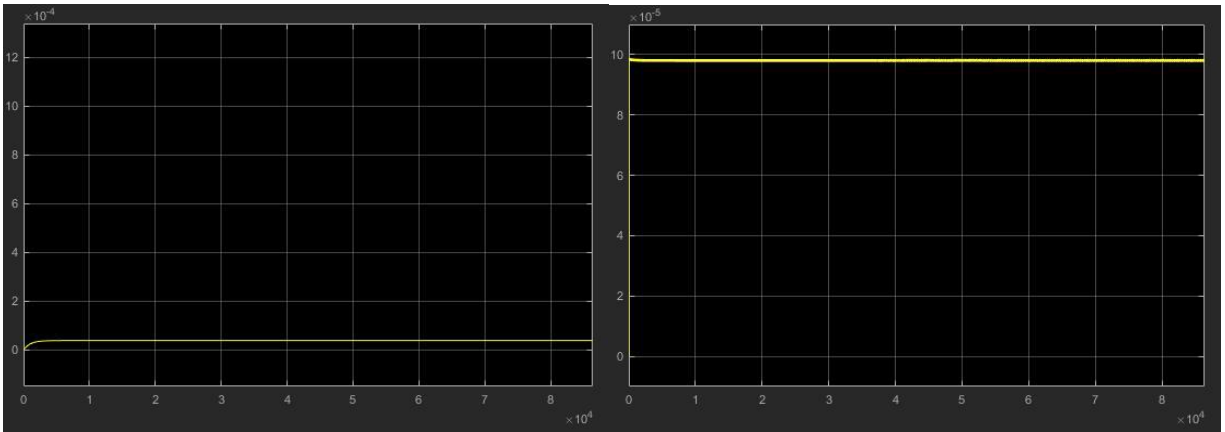


Figure 9. The same order of plots is displayed as in Figure 7 for a RAVE value of 1. The development of tolerance is significantly inhibited by the use of an agonist which promotes rapid internalization following phosphorylation. Time axis is in seconds.

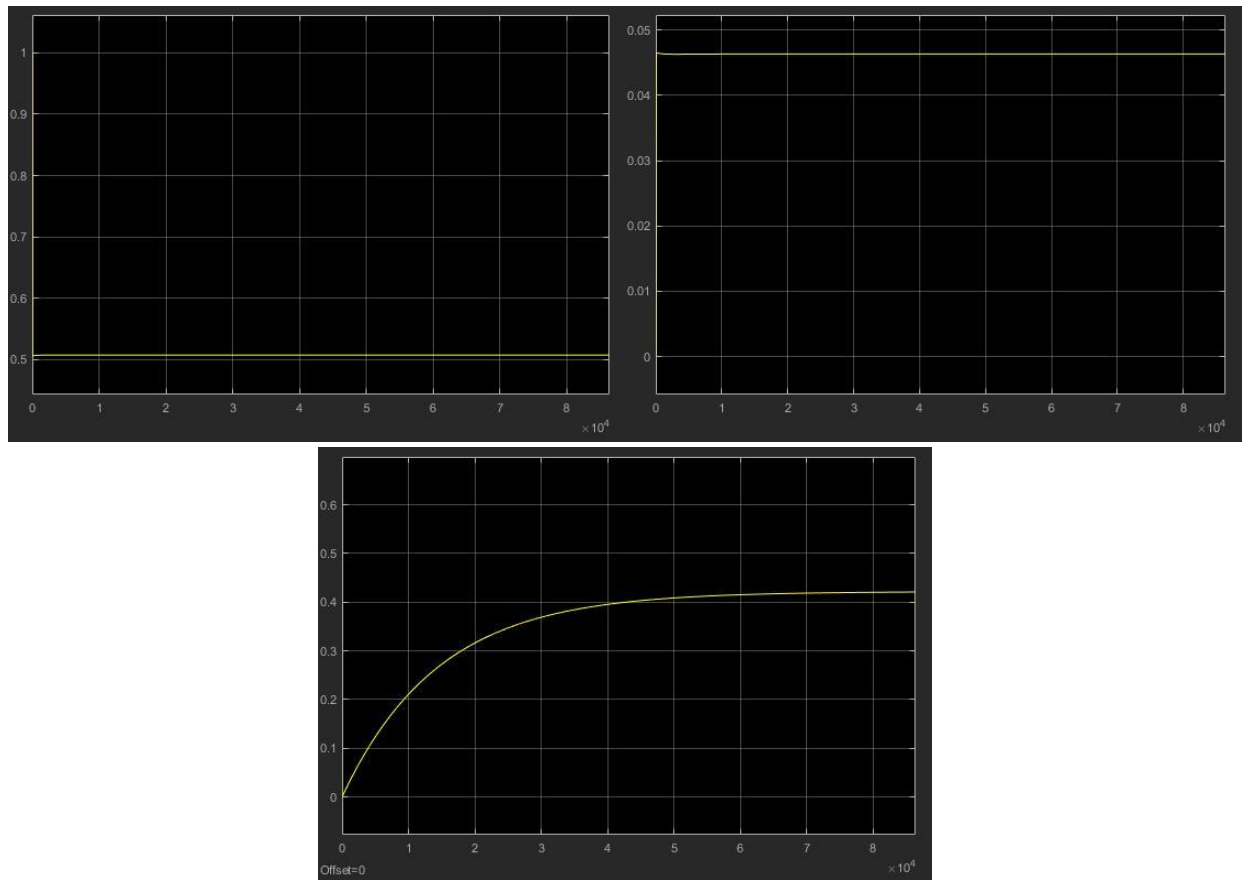


Figure 10. Resultant cellular responses to lack of tolerance in the μ opioid receptor response. Calcium (top left), GIRK (top right), and AMPA (bottom) currents reach steady-state values by the end of a day which remain constant due to the activation of more G proteins from the steady-state opioid receptor values. Time axis is in seconds.

Discussion

The above model is found to accurately reproduce the dynamic effects of μ opioid receptor activation with morphine on both acute and chronic time scales, by considering suppression of transmitter release by inhibition of calcium currents, activation of G protein-coupled potassium currents, and internalization of dendritic AMPA receptors. The development of tolerance is introduced based on the RAVE parameter, which highlights the tendency of agonists like morphine to promote tolerance, while those such as DHE do not. Magnitudes for some of the outputs deviate slightly from expected values, and for other outputs, the current literature is lacking in quantification.

This deviation may be due to several reasons, including the relative novelty of examining specific intracellular actions of opioid receptor activation and the inability to decouple intracellular opioid transduction pathways from other cellular events. G proteins are a ubiquitous second messenger in signal transduction, and it is therefore quite difficult to quantify the specific temporal behavior of G protein dynamics only as a consequence of μ opioid receptor activation. This also means that other influxes and effluxes of G proteins from different signal reception may alter observed activation and deactivation kinetics. This is just one example of the complexity of isolating specific intracellular circuits, and as the opioid receptor families have been found to stimulate a large number of pathways beyond those considered here, deviations are expected.

Intracellular levels of cyclic AMP have been studied in depth in relation to the regulation of opioid receptor activity and the development of tolerance. It has been hypothesized that ineffective regulation of cAMP pathways may be a contributor to opioid tolerance. In this hypothesis, upregulation of adenylyl cyclase, protein kinase A, and CREB, a protein which binds to the cAMP response element on DNA, may offset the effects of inhibitory G protein activation by opioids [12]. The β arrestin family, which is involved in internalization of μ opioid receptors, is also believed to be an important downstream factor in regulation of tolerance. Activation of different members of this family (e.g. β arrestin 1 vs. 2) may be one of the mechanisms by which different agonists mediate functional selectivity [12]. The action of protein kinase C has also been found to mediate receptor phosphorylation, desensitization, and internalization [24].

While the above model follows the hypothesis that receptor inactivation/desensitization is the first step in the development of tolerance, and that the RAVE parameter only affects steps downstream in this pathway (i.e. endocytosis), some evidence in the literature suggests that there may not be an explicit link between desensitization and tolerance [13, 31]. In fact, morphine has been believed to promote only minimal acute desensitization, though studies have found development of morphine-dependent desensitization. However, tolerance and desensitization in these studies are shown to be reversed by the presence of different signaling proteins and enzymes, suggesting distinct cellular pathways. Receptor downregulation is also not considered in the above model, but has been observed *in vitro* [32] and *in vivo* [33].

Ultimately, the biology of μ opioid receptor activation and subsequent development of opioid tolerance is far more complex than that reproduced in the above model, and will likely further increase in complexity as subsequent investigations are conducted in the coming years.

Even so, the above model reproduces the expected cellular behavior from morphine exposure, and highlights some of the fundamental intracellular mediators of the acute and chronic responses to morphine. Certainly, the actual underlying mechanisms of agonist functional selectivity must be uncovered to properly capture development of tolerance from some ligands but not from others, but the RAVE parameter is sufficient in characterizing this selectivity from a phenomenological standpoint. Introduction of other known molecular participants in opioid signal transduction will serve to further improve the model and more accurately reproduce the magnitude and time course of tolerance.

Conclusions

A model has been constructed in Simulink in order to examine the dynamics of the μ opioid receptor on regulating the analgesic effects of morphine and the rapid development of morphine tolerance. The neuronal basis is introduced based on kinetic models for NMDA, AMPA, and GABA_A receptors in the dendrites, the Hodgkin-Huxley model in the axon, an m^2h Hodgkin-Huxley-like model for Ca^{2+} current, and a simple kinetic model for transmitter release from existing literature. The opioid dependence is introduced using a four-state kinetic model for the receptor, considering free, bound, phosphorylated/desensitized, and internalized receptors. The former two states regulate the activation of G proteins, which mediate many of the intracellular effects of opioid receptor activation, including suppression of calcium influx by channel phosphorylation, activation of hyperpolarizing potassium currents via GIRK channels, and AMPA receptor internalization. The latter two states mediate the inactivation/activation dynamics of the receptors by considering the experimental RAVE parameter, which has been shown to be correlated with the development of tolerance.

This model examines one of many current hypotheses regarding the development of tolerance in the opioid system. There is little debate that the μ opioid receptor is the primary mediator of the reduced cellular response to prolonged morphine exposure, and that this response involves changes in the functional state of the receptor. A number of assumptions were used in the above model which may result in deviations from observed cellular effects, but the dynamics have been found to agree well with experimental data. Certainly, modifications or additions may be made to the model to more accurately capture dynamics of opioid activity, but the current state is largely successful in considering the role of G protein activation in mediating analgesia and tolerance.

References

1. Kandel, E.R., et al., *Principles of Neural Science, Fifth Edition*. 2012: McGraw-Hill Education.
2. Stuart, G., et al., *Action potential initiation and backpropagation in neurons of the mammalian CNS*. Trends in Neurosciences, 1997. **20**(3): p. 125-131.
3. Snutch, T.P., et al. *Molecular Properties of Voltage-Gated Calcium Channels*. 2004.
4. Contet, C., B.L. Kieffer, and K. Befort, *Mu opioid receptor: a gateway to drug addiction*. Curr Opin Neurobiol, 2004. **14**(3): p. 370-8.
5. Moises, H.C., K.I. Rusin, and R.L. Macdonald, *mu-Opioid receptor-mediated reduction of neuronal calcium current occurs via a G(o)-type GTP-binding protein*. J Neurosci, 1994. **14**(6): p. 3842-51.
6. Wilding, T.J., M.D. Womack, and E.W. McCleskey, *Fast, local signal transduction between the mu opioid receptor and Ca²⁺ channels*. J Neurosci, 1995. **15**(5 Pt 2): p. 4124-32.
7. Ikeda, K., et al., *Involvement of G-protein-activated inwardly rectifying K (GIRK) channels in opioid-induced analgesia*. Neurosci Res, 2000. **38**(1): p. 113-6.
8. Lüscher, C. and P.A. Slesinger, *Emerging concepts for G protein-gated inwardly rectifying potassium (GIRK) channels in health and disease*. Nature reviews. Neuroscience, 2010. **11**(5): p. 301-315.
9. Torrecilla, M., et al., *G-Protein-Gated Potassium Channels Containing Kir3.2 and Kir3.3 Subunits Mediate the Acute Inhibitory Effects of Opioids on Locus Ceruleus Neurons*. The Journal of Neuroscience, 2002. **22**(11): p. 4328-4334.
10. Kam, A.Y., et al., *Morphine induces AMPA receptor internalization in primary hippocampal neurons via calcineurin-dependent dephosphorylation of GluR1 subunits*. J Neurosci, 2010. **30**(45): p. 15304-16.
11. Vekovischeva, O.Y., et al., *Morphine-induced dependence and sensitization are altered in mice deficient in AMPA-type glutamate receptor-A subunits*. J Neurosci, 2001. **21**(12): p. 4451-9.
12. Al-Hasani, R. and M.R. Bruchas, *Molecular mechanisms of opioid receptor-dependent signaling and behavior*. Anesthesiology, 2011. **115**(6): p. 1363-81.
13. Borgland, S.L., *Acute opioid receptor desensitization and tolerance: is there a link?* Clin Exp Pharmacol Physiol, 2001. **28**(3): p. 147-54.
14. Finn, A.K. and J.L. Whistler, *Endocytosis of the mu opioid receptor reduces tolerance and a cellular hallmark of opiate withdrawal*. Neuron, 2001. **32**(5): p. 829-39.
15. Hayhurst, C.J. and M.E. Durieux, *Differential Opioid Tolerance and Opioid-induced Hyperalgesia: A Clinical Reality*. Anesthesiology, 2016. **124**(2): p. 483-488.
16. Destexhe, A., Z. Mainen, and T. Sejnowski, *Kinetic Models of Synaptic Transmission*. Vol. 2. 1998. 1-26.
17. Gerstner, W., et al., *Neuronal Dynamics: From Single Neurons to Networks and Models of Cognition*. 2014: Cambridge University Press. 568.
18. De Schutter, E., *Computational Neuroscience: Realistic Modeling for Experimentalists*. 2000: CRC Press.
19. Destexhe, A., et al., *A model of spindle rhythmicity in the isolated thalamic reticular nucleus*. J Neurophysiol, 1994. **72**(2): p. 803-18.
20. Prinz, J.-H., et al., *Markov models of molecular kinetics: Generation and validation*. The Journal of Chemical Physics, 2011. **134**(17): p. 174105.
21. Capogna, M., B.H. Gähwiler, and S.M. Thompson, *Mechanism of mu-opioid receptor-mediated presynaptic inhibition in the rat hippocampus in vitro*. J Physiol, 1993. **470**: p. 539-58.
22. Rusin, K.I. and H.C. Moises, *mu-Opioid receptor activation reduces multiple components of high-threshold calcium current in rat sensory neurons*. J Neurosci, 1995. **15**(6): p. 4315-27.
23. Liao, D., et al., *Mu-opioid receptors modulate the stability of dendritic spines*. Proceedings of the National Academy of Sciences of the United States of America, 2005. **102**(5): p. 1725-1730.

24. Ueda, H. and M. Ueda, *Mechanisms underlying morphine analgesic tolerance and dependence*. Front Biosci (Landmark Ed), 2009. **14**: p. 5260-72.
25. Williams, J.T., et al., *Regulation of mu-opioid receptors: desensitization, phosphorylation, internalization, and tolerance*. Pharmacol Rev, 2013. **65**(1): p. 223-54.
26. Martini, L. and J.L. Whistler, *The role of mu opioid receptor desensitization and endocytosis in morphine tolerance and dependence*. Current Opinion in Neurobiology, 2007. **17**(5): p. 556-564.
27. Kapoor, A., et al., *Dynamic and Kinetic Elements of μ -Opioid Receptor Functional Selectivity*. Scientific Reports, 2017. **7**(1): p. 11255.
28. Wang, Y.H., et al., *Paradoxical relationship between RAVE (relative activity versus endocytosis) values of several opioid receptor agonists and their liability to cause dependence*. Acta Pharmacol Sin, 2010. **31**(4): p. 393-8.
29. Wydeven, N., et al., *Mechanisms underlying the activation of G-protein-gated inwardly rectifying K⁺ (GIRK) channels by the novel anxiolytic drug, ML297*. Proceedings of the National Academy of Sciences, 2014. **111**(29): p. 10755-10760.
30. Bourinet, E., et al., *Determinants of the G protein-dependent opioid modulation of neuronal calcium channels*. Proceedings of the National Academy of Sciences of the United States of America, 1996. **93**(4): p. 1486-1491.
31. Levitt, E.S. and J.T. Williams, *Morphine Desensitization and Cellular Tolerance Are Distinguished in Rat Locus Ceruleus Neurons*. Molecular Pharmacology, 2012. **82**(5): p. 983-992.
32. Law, P.Y., D.S. Hom, and H.H. Loh, *Loss of opiate receptor activity in neuroblastoma X glioma NG108-15 hybrid cells after chronic opiate treatment. A multiple-step process*. Mol Pharmacol, 1982. **22**(1): p. 1-4.
33. Bernstein, M.A. and S.P. Welch, *mu-Opioid receptor down-regulation and cAMP-dependent protein kinase phosphorylation in a mouse model of chronic morphine tolerance*. Brain Res Mol Brain Res, 1998. **55**(2): p. 237-42.